

source of the efficient mixing in the presence of chaotic advection. This phenomenon is being exploited in various procedures for mixing highly viscous fluids, including applications to materials processing, in micro-fluidics, and even in large-scale atmospheric, oceanographic, and geological flows. It may play a role in the feeding of microorganisms.

In the case of 2-d incompressible flows the equations of motion allow for an interesting connection to Hamiltonian dynamics. The velocity field can be represented through a stream function $\psi(x, y, t)$, so that $\mathbf{u} = \nabla \times \psi \mathbf{e}_z$ and Equations (1) for the trajectories of fluid elements become

$$\dot{x} = \frac{\partial \psi}{\partial y}, \quad \dot{y} = -\frac{\partial \psi}{\partial x}. \quad (2)$$

The relation to Hamilton's canonical equations is established through the identification x =position, y =momentum, and ψ =Hamilton function. Thus, what is the phase space in Hamiltonian systems can be visualized as the position space in the hydrodynamic situation. The structures that appear in 2-d periodically driven flows are, therefore, similar to the phase space structures in a Poincaré surface of section for a chaotic Hamiltonian system, and the same techniques can be used to analyze the transport of particles and the stretching and folding of material lines.

The phenomena that arise in chaotic advection by simple flows may be relevant to turbulent flows when a separation of length and time scales is possible. Consider, for example, the small-scale structures that appear in the density of a tracer substance when the molecular diffusivity κ of the tracer is much smaller than the kinematic viscosity ν of the liquid, that is, in a situation where the Schmidt number $Sc = \nu/\kappa$ is much larger than one. Then, the velocity field is smooth below the Kolmogorov scale, $\lambda_K = (\nu^3/\varepsilon)^{1/4}$, where ε is the kinetic energy dissipation, but the scalar field has structures on even smaller scales, down to $\lambda_s = (Sc)^{-1/2} \lambda_K$. These arise from Lagrangian chaos with a randomly fluctuating velocity field. The patterns produced in this so-called Batchelor regime are strikingly similar to the ones observed in laminar flows.

On larger scales, ideas from chaotic advection are relevant when there are large-scale coherent structures with slow spatial and temporal evolution. Typical examples are 2-d or quasi-2-d flows, for example, in the atmosphere or in the oceans. Fluid volumes can be trapped in regions bounded by separatrices or by stable and unstable manifolds of stagnation points and may have very little exchange with their surroundings. Such a reduction in stirring appears to occur in the Wadden sea (Ridderinkhof & Zimmerman, 1992).

Equations (1) apply in this form to fluid elements and ideal particles only. For realistic particles with finite volume and inertia, further terms must be added. A

significant change in the qualitative side is that the effective velocity field for inertial particles can have a nonvanishing divergence even for incompressible flows (Maxey & Riley, 1983).

The book by Ottino, (1989) and the two conference proceedings (Aref, 1994; IUTAM, 1991) provide good starting points for entering the many aspects of chaotic advection and Lagrangian chaos in engineering applications, geophysical flows, turbulent flows, and theoretical modeling. Historical remarks may be found in the Introduction to Aref, (1994) and in Aref, (2002). Today, the term chaotic advection designates an established subtopic of fluid mechanics that is used as a classification keyword by leading journals and conferences in the field.

HASSAN AREF AND BRUNO ECKHARDT

See also **Chaotic dynamics; Chaos vs. turbulence; Dynamical systems; Hamiltonian systems; Lyapunov exponents; Turbulence**

Further Reading

- Aref, H. 1984. Stirring by chaotic advection. *Journal of Fluid Mechanics*, 143: 1–21
- Aref, H. (editor). 1994. Chaos applied to fluid mixing. *Chaos, Solitons and Fractals*, 4: 1–372
- Aref, H. 2002. The development of chaotic advection. *Physics of Fluids*, 14: 1315–1325
- IUTAM Symposium on fluid mechanics of stirring and mixing. 1991. *Physics of Fluids*, 3: 1009–1496
- Maxey, M. & Riley, J. 1983. Equation of motion for a small rigid sphere in a nonuniform flow. *Physics of Fluids*, 26: 883–889
- Ottino, J.M. 1989. *The Kinematics of Mixing: Stretching, Chaos and Transport*, Cambridge: Cambridge University Press
- Ridderinkhof, H. & Zimmermann, J.T.F. 1992. Chaotic stirring in a tidal system. *Science*, 258: 1107–1111

CHAOTIC BILLIARDS

See **Billiards**

CHAOTIC DYNAMICS

When we say “chaos”, we usually imagine a very complex scene with many different elements that move in different directions, collide with each other, and appear and disappear randomly. Thus, according to everyday intuition, the system's complexity (e.g., many degrees of freedom) is an important attribute of chaos. It seems reasonable to think that in the opposite case, for example, a system with only a few degrees of freedom, the dynamical behavior must be simple and predictable. In fact, this point of view is Laplacian determinism.

The discovery of dynamical chaos has destroyed this traditional view. Dynamical chaos is a phenomenon that can be described by mathematical models for many natural systems, for example, physical, chemical, biological, and social, which evolve in time according to a deterministic rule and demonstrate capricious and

seemingly unpredictable behavior. To illustrate such behavior, consider a few examples.

Examples

Hyperion: Using Newton’s laws, one can compute relatively easily all future solar eclipses not only for the next few hundred years but also for thousands and millions of years into the future. This is indicative of a real predictability of the system’s dynamical behavior. But even in the solar system, there exists an object with unpredictable behavior: a small irregularly shaped moon of Saturn, Hyperion. Its orbit is regular and elliptic, but its altitude in the orbit is not. Hyperion is tumbling in a complex and irregular pattern while obeying the laws of gravitational dynamics. Hyperion may not be the only example of chaotic motion in the solar system. Recent studies indicate that chaotic behavior possibly exists in Jovian planets (Murray & Holman, 1999), resulting from the overlap of components of the mean motion resonance among Jupiter, Saturn, and Uranus. Chaos in Hamiltonian systems, which represent the dynamics of the planets, arises when one resonance is perturbed by another one (See **Standard map**).

Chaotic mixing is an example of the complex irregular motion of particles in a regular periodic velocity field, like drops of cream in a cup of coffee; see Figure 1. Such mixing, caused by sequential stretching and folding of a region of the flow, illustrates the general mechanism of the origin of chaos in the phase space of simple dynamical systems (See **Mixing**).

Billiards: For its conceptual simplicity, nothing could be more deterministic and completely predictable

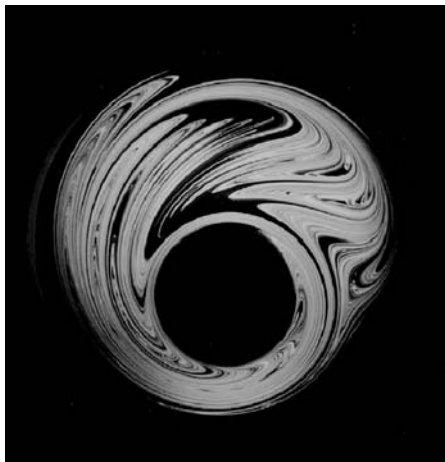


Figure 1. Mixing of a passive tracer in a Newtonian flow between two rotating cylinders with different rotation axes. The rotation speed of the inner cylinder is modulated with constant frequency. The flow is stretched and folded in a region of the flow. The repetition of these operations leads to a layered structure—folds within folds, producing a fractal structure (Ottino, 1989).

than the motion of a single ball on a billiard table. However, in the case of a table bounded by four quarters of a circle curved inward (Sinai billiard), the future fate of a rolling billiard ball is unpredictable beyond a surprisingly small number of bounces. As indicated by Figure 2, a typical trajectory of the Sinai billiard is irregular and a statistical approach is required for a quantitative description of this simple mechanical system. Such an irregularity is the result of having a finite space and an exponential instability of individual trajectories resulting in a sensitive dependence on initial conditions.

Due to the curved shape of the boundary, two trajectories emanating from the same point but in slightly different directions with angle δ between them, hit the boundary $\partial\Omega$ (see Figure 2) at different points that are $c\delta$ apart where $c > 0$. After a bounce, the direction of the trajectories will differ by angle $(1 + 2c)\delta$, and because an actual difference between the directions is multiplied by a factor $\mu = (1 + 2c) > 1$, the small perturbation δ will grow more or less exponentially (Sinai, 2000). Such sensitive dependence on initial conditions is the main feature of every chaotic system.

A Markov map: To understand in more detail how randomness appears in a nonrandom system, consider a simple dynamical system in the form of a one-dimensional map

$$x_{n+1} = 2x_n \text{ mod } 1. \tag{1}$$

Since the distance between any two nearby trajectories ($|x_n - x'_n| \ll 1$) after each iteration increases at least two times ($|dx_{n+1}/dx_n| = 2$), any trajectory of the map is unstable. The map has a countable infinity of unstable periodic trajectories, which can be seen as fixed points when one considers the shape of the map $x_{n+k} = F^{(k)}(x_n)$; see Figure 3(b). Since all fixed points and periodic trajectories are repelling, the only possibility left for the most arbitrarily selected initial condition is that the map will produce a chaotic motion that never exactly repeats itself. The irregularity of such dynamics can be illustrated using a binary symbolic description ($s_n = 0$ if $x_n < \frac{1}{2}$ and $s_n = 1$ if $x_n \geq \frac{1}{2}$). In this case, any value of x_n can be represented as a binary

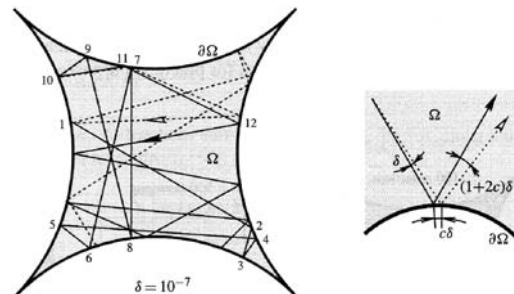


Figure 2. Illustration of the trajectory sensitivity to the initial conditions in a billiard model with convex borders.

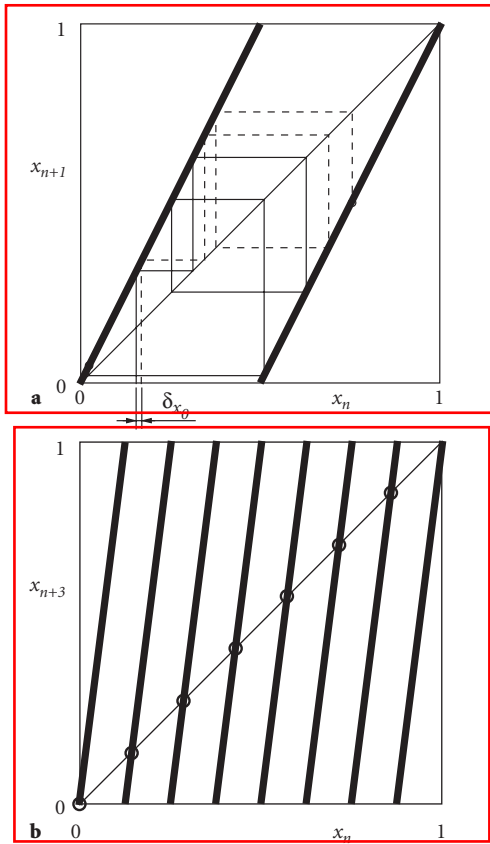


Figure 3. Simple map diagram: (a) two initially close trajectories diverge exponentially; (b) illustration of the increasing of the number of unstable periodic trajectories with the number of iterations.

decimal

$$x_n = 0.s_{n+1}s_{n+2}s_{n+3}\dots \equiv \sum_{j=n+1}^{\infty} 2^{-j}s_j.$$

If the initial state happens to be a rational number, it can be written as a periodic sequence of 0's and 1's. For instance, $0.10111011101110111\dots$ is the rational number $\frac{11}{15}$. Each iteration $x_n \rightarrow x_{n+1}$ of map (1) corresponds to setting the symbol s_{n+1} to zero and then moving the decimal point one space to the right (this is known as a *Bernoulli shift*). For example, the iterations of the number $\frac{11}{15}$ yield

$$\begin{aligned} &0.10111011101110111\dots, \\ &0.01110111011101110\dots, \\ &0.11101110111011101\dots, \\ &0.11011101110111011\dots, \\ &0.10111011101110111\dots, \end{aligned}$$

which illustrates a periodic motion of period 4. Selecting an irrational number as the initial condition, one chooses a binary sequence that cannot be split into groups of 0's and 1's periodically repeated an infinite number of times. As a result, each iteration of the

irrational number generates a new irrational number. Since the irrational numbers appear in the interval $x_n \in [0, 1]$ with probability one, one can observe only the aperiodic (chaotic) motions. Random-like behavior of the chaotic motions is illustrated in a separate figure in the color plate section (See the color plate section for a comparison of chaos generated by Equation (1) and a truly random process).

The degree of such chaoticity is characterized by *Lyapunov exponents* that can be defined for one-dimensional maps ($x_{n+1} = f(x_n)$). The stability or instability of a trajectory with the initial state x_0 is determined by the evolution of neighboring trajectories starting at $\tilde{x}_0 = x_0 + \delta x_0$ with $|\delta x_0| \ll 1$. After one iteration

$$\tilde{x}_1 = x_1 + \delta x_1 = f(x_0 + \delta x_0) \approx f(x_0) + \left. \frac{df}{dx} \right|_{x=x_0} \delta x_0.$$

Now, the deviation is $\delta x_1 \approx f'(x_0)\delta x_0$. After the n th iteration it becomes $\delta x_n = (\prod_{m=0}^{n-1} f'(x_m))\delta x_0$. The evolution of the distance between the two trajectories is calculated by taking the absolute value of this product. For infinitesimally small perturbations and large enough n , it is expected that $|\delta x_n| = \alpha^n |\delta x_0|$, where

$$\alpha \approx \lim_{n \rightarrow \infty} \left(\left| \frac{\delta x_n}{\delta x_0} \right| \right)^{1/n} = \left(\prod_{m=0}^{n-1} |f'(x_m)| \right)^{1/n}$$

or

$$\ln \alpha \approx \lambda = \lim_{n \rightarrow \infty} \frac{1}{n} \sum_{m=0}^{n-1} \ln (|f'(x_m)|). \quad (2)$$

Limit (2) exists for a typical trajectory x_m and defines the Lyapunov exponent, λ , which is the time average of the rate of exponential divergence of nearby trajectories. For map (1) $f' = 2$ for all values of x and, therefore, $\lambda = \ln 2$ (See **Lyapunov exponents**).

Assuming that the initial state cannot be defined with absolute accuracy, the prediction of the state of the map after a sufficiently large number of iterations becomes impossible. The only description that one can use for defining that state is a statistical one. The statistical ensemble in this case is the ensemble of initial conditions. The equation of evolution for the initial state probability density $\rho_{n+1}(F(x))$ can be written as (Ott, 1993, p. 33)

$$\rho_{n+1}(F(x)) = \sum_{j=1,2} \rho_n(x) \left| \frac{dF(x)}{dx} \right|_j, \quad (3)$$

where the summation is taken over both branches of $F(x)$. Considering the evolution of a sharp initial distribution $\rho_0(x)$, one can see that at each step this distribution becomes smoother. As n approaches infinity, the distribution asymptotically approaches the steady state $\rho(x) = 1$.

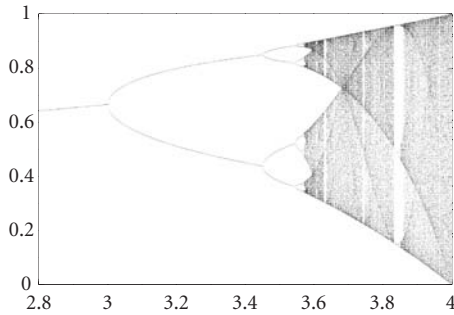


Figure 4. Bifurcation diagram for the logistic map.

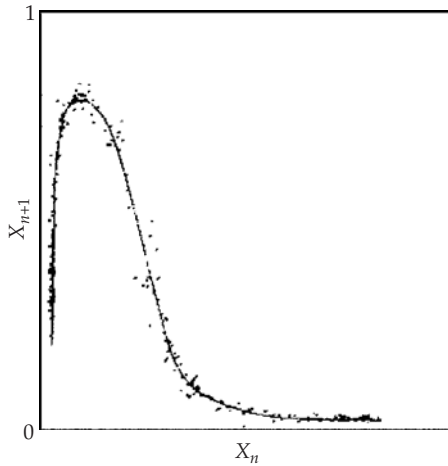


Figure 5. Return map measured in the Belousov-Zhabotinsky autocatalytic reaction.

Population dynamics: A popular model of population growth is the logistic map $x_{n+1} = \alpha x_n(1 - x_n)$, $0 \leq \alpha \leq 4$ (See **Population dynamics**). The formation of chaos in this map is illustrated in the bifurcation diagram shown in Figure 4. This diagram presents the evolution of the attracting set as the value of α grows. Below the Feigenbaum point $\alpha_\infty = 3.569 \dots$, the attractor of the map is periodic. Its period increases through a sequence of period-doubling bifurcations as the value of α approaches α_∞ (See **Period doubling**). For $\alpha > \alpha_\infty$, the behavior is chaotic but some windows of periodic attractors exist (See **Order from chaos**).

Belousov-Zhabotinsky (BZ) autocatalytic reaction: In the BZ reaction (See **Belousov-Zhabotinsky reaction**), an acid bromate solution oxidizes malonic acid in the presence of a metal ion catalyst and other important chemical components in a well-stirred

reactor (Roux et al., 1983). The concentration of the bromide ions is measured and parameterized by the return map (plotting a variable against its next value in time) $x_{n+1} = \alpha x_n \exp[-bx_n]$ (see Figure 5). This map exhibits chaotic behavior for a very broad range of parameter values.

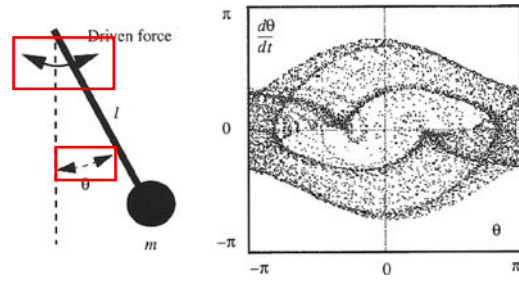


Figure 6. Chaotic oscillation of a periodically driven pendulum, in phase-space plot of angular velocity versus angular position (Deco & Schürmann, 2000).

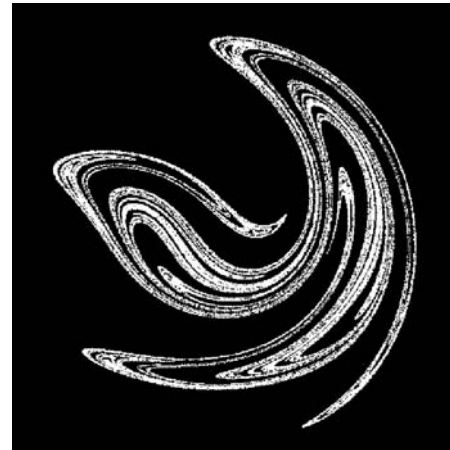


Figure 7. Ueda attractor. The fractal structure of the attractor is typical for all chaotic sets (compare this picture with Figure 1) (Ueda, 1992).

Simple chaotic oscillators: The dynamics of the periodically driven pendulum shown in Figure 6 is described by

$$\frac{d^2\Theta}{dt^2} + \nu \frac{d\Theta}{dt} + \frac{g}{l} \sin \Theta = B \cos 2\pi f t, \quad (4)$$

where the term on the right-hand side is the forcing (sinusoidal torque) applied to the pivot and f is the forcing frequency. Chaotic motions of the pendulum computed for $\nu = 0.5$, $g/l = 1$, $B = 1.15$, $f = 0.098$, and visualized with stroboscopic points at moments of time $t = i/f$ are shown in Figure 6.

A similar example of chaotic behavior was intensively studied in an oscillator where the restoring force is proportional to the cube of the displacement (Ueda, 1992, p. 158)

$$\frac{d^2\Theta}{dt^2} + \nu \frac{d\Theta}{dt} + \Theta^3 = B \cos t. \quad (5)$$

The stroboscopic image (with $t = i$) of the strange attractor in this forced Duffing-type oscillator computed with $\nu = 0.05$ and $B = 7.5$ is shown in Figure 7.

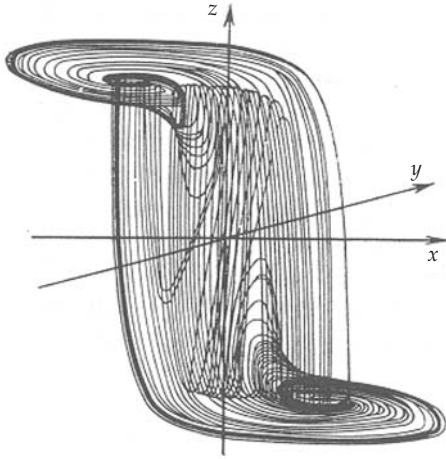


Figure 8. Chaotic attractor generated by electric circuit, which is a modification of van der Pol oscillator: $\dot{x} = hx + y - gz$; $\dot{y} = -x$; $\mu\dot{z} = x - f(x)$; where $f(x) = x^3 - x$ (Pikovsky & Rabinovich, 1978).

Figure 8 presents a chaotic attractor generated by an electronic circuit. Such circuits are a popular topic in engineering studies today.

Characteristics of Chaos

Lyapunov exponents: Consider the Lyapunov exponents for a trajectory $\tilde{x}(t)$ generated by a d -dimensional autonomous system

$$\frac{d\mathbf{x}}{dt} = \mathbf{F}(\mathbf{x}), \quad (6)$$

with initial condition \mathbf{x}_0 , $\mathbf{x} \in \mathfrak{R}^d$. Linearizing Equation (6) about this solution, one obtains a linear system which describes the evolution of infinitesimally small perturbations $\mathbf{w} = \mathbf{x}(t) - \tilde{\mathbf{x}}(t)$ of the trajectory, in the form

$$\frac{d\mathbf{w}}{dt} = \mathbf{M}(\tilde{\mathbf{x}})\mathbf{w}, \quad (7)$$

where $\mathbf{M}(\mathbf{x}) = \partial\mathbf{F}(\mathbf{x})/\partial\mathbf{x}$ is the Jacobian of $\mathbf{F}(\mathbf{x})$ that changes in time in accordance with $\tilde{\mathbf{x}}(t)$. In d -dimensional phase space of (7), consider a sphere of initial conditions for perturbations $\mathbf{w}(t)$ of diameter l , that is, $|\mathbf{w}(0)| \leq l$. The evolution of this ball in time is governed by linear system (7) and depends on trajectory $\tilde{\mathbf{x}}(t)$. As the system evolves in time, the ball transforms into an ellipsoid. Let the ellipsoid have d principal axes of different length l_j , $j = 1, d$. Then, the values of Lyapunov exponents of the trajectory $\tilde{\mathbf{x}}(t)$ are defined as

$$\lambda_j(\tilde{\mathbf{x}}) = \lim_{t \rightarrow \infty} \left[\left(\frac{1}{t} \right) \ln \left(\frac{l_j(\tilde{\mathbf{x}}, t)}{l(\mathbf{x}_0, 0)} \right) \right]. \quad (8)$$

Although limit (8) depends on $\tilde{\mathbf{x}}(t)$, the *spectrum of the Lyapunov exponents* λ_j for the selected regime of

chaotic oscillations generated by (6) is independent of the initial conditions for the typical trajectories and characterizes the chaotic behavior.

The Lyapunov exponents, λ_j , can be ordered in size: $\lambda_1 \geq \lambda_2 \geq \dots \geq \lambda_d$. Self-sustained oscillations in autonomous time-continuous systems always have at least one Lyapunov exponent that is equal to zero. This is the exponent characterizing the stretching of phase volume along the trajectory. The spectrum of λ_j for chaotic trajectories contains one or more Lyapunov exponents with positive values.

Kolmogorov–Sinai entropy is a measure of the degree of predictability of further states visited by a chaotic trajectory started within a small region. Due to the divergence, a long-term observation of such a trajectory gives more and more information about the actual initial condition of the trajectory. In this sense, one may say that a chaotic trajectory creates information. Consider a partitioning of the d -dimensional phase space into small cubes of volume ε^d . Observing a continuous trajectory during T instances of time, one obtains a sequence $\{i_0, i_1, \dots, i_T\}$, where i_0, i_1, \dots are the indexes of the cubes consequently visited by the trajectory. As a result, the type of the trajectory observed during the time interval from 0 to T is specified by the sequence $\{i_0, i_1, \dots, i_T\}$. As Kolmogorov and Sinai showed, in dynamical systems whose behavior is characterized by exponential instability, the number of different types of trajectories, K_T , grows exponentially with T :

$$0 < H = \lim_{T \rightarrow \infty} \frac{1}{T} \log K_T.$$

The quantity H is the Kolmogorov–Sinai (KS) entropy.

The number of unique random sequences $\{i_0, i_1, \dots, i_T\}$ that can be obtained without any rules applied increases exponentially with T . In the case of nonrandom sequences where there is a strict law for the generation of future symbols, like the periodic motion, the number of possible sequences grows in time slower than the exponent. Since the exponential growth takes place for the segments of trajectories in the unstable dynamical system producing chaos, such a dynamical system is capable of generating “random” sequences. The Kolmogorov–Sinai entropy is a measure of such “randomness” in a “nonrandom” system, for example, a dynamical system.

Since both KS entropy and Lyapunov exponents reflect the properties of the divergence of the nearby trajectories, these characteristics are related to each other. The formula describing this relation is given by Ruelle’s Inequality

$$H \leq K = \sum_{j=1}^m \lambda_j \geq 0 \quad (9)$$

where m is the number of positive λ_i ($K_2 = 0$, when $m = 0$). The equality $H = K$ holds when the system

has a physical measure (Sinai–Ruelle–Bowen measure) (Young, 1998). The invariant set of trajectories characterized by a positive Kolmogorov–Sinai entropy is a chaotic set.

Forecasting

If a sufficiently long experimental time series capturing the chaotic process of an unknown dynamical system is available in the form of scalar data $\{x_n\}_{n=0}^N$, it is possible, in principle, to predict x_{N+m} with finite accuracy for some $m \geq 1$. Such predictions are based on the assumption that the unknown generating mechanism is time independent. As a result, “what happened in the past may happen again—even stronger: that what is happening now has happened in the past” (Takens, 1991). In classical mechanics (no dissipation), this idea of “what happens now has happened in the past” is related to the Poincaré Recurrence Theorem.

Usually, the prediction procedure consists of two steps: first, it is necessary to consider all values of n in the “past,” that is, with $n < N$, such that $\sum_{k=0}^K |x_{n-k} - x_{N-k}| < \varepsilon$, where ε is a small constant. If there are only a few of such n , then one can try again with a smaller value of K or a larger value of ε . In the second step, it is necessary to consider the corresponding elements x_{n+l} for all the values of n found in the first step. Finally, taking a union of the ε -neighborhoods of all these elements, one can predict that x_{N+l} will be in this union.

To understand when and why forecasting is possible and when it is not, it is reasonable to use characteristics such as *dimension* and *entropy* that can be computed directly from time series (Takens, 1991). If we want to make a catalog of essentially different segments of length $k + 1$ in $\{x_n\}_{n=0}^N$, this can be done with $C(k, \varepsilon, N)$ elements. $C(k, \varepsilon, N)$ is a function of N that has a limit $C(k, \varepsilon) = \lim_{N \rightarrow \infty} C(k, \varepsilon, N)$, and for prediction, we need $C(k, \varepsilon) \ll N$.

The quantitative measure for the way in which $C(k, \varepsilon)$ increases as ε goes to zero is

$$D = \lim_{k \rightarrow \infty} \left(\frac{\lim_{\varepsilon \rightarrow 0} C(k, \varepsilon, N)}{\ln(1/\varepsilon)} \right). \tag{10}$$

If D is large, the prediction is problematic. The quantity D defined by (10) is the dimension of the time series.

The quantitative measure for the way in which $C(k, \varepsilon)$ increases with k is

$$H = \overline{\lim}_{\varepsilon \rightarrow 0} \left(\lim_{k \rightarrow \infty} \frac{C(k, \varepsilon, N)}{k} \right), \tag{11}$$

This is the entropy of the time series. For the time series generated by a differentiable dynamical system, both the dimension and entropy are finite, but for a random time series they are infinite. Suppose each x_n is taken at

random in the interval $[0, 1]$ (with respect to the uniform distribution) and for each n_1, \dots, n_k (different), the choices of x_{n_1}, \dots, x_{n_k} are independent. For such time series, one can find: $C(k, \varepsilon) = (1 + \lfloor 1/2\varepsilon \rfloor)^{k+1}$, where $\lfloor 1/2\varepsilon \rfloor$ is the integer part of $1/2\varepsilon$. From this formula, it immediately follows that both dimension and entropy in such random time series are infinite.

Models of the Earth’s atmosphere are generally considered as chaotic dynamical systems. Due to the unstability, even infinitesimally small uncertainties in the initial conditions grow exponentially fast and make a forecast useless after a finite time interval. This is known as the butterfly effect. However, in the tropics, there are certain regions where wind patterns and rainfall are so strongly determined by the temperature of the underlying sea surface, that they do not show such sensitive dependence on the atmosphere. Therefore, it should be possible to predict large-scale tropical circulation and rainfall for as long as the ocean temperature can be predicted (Shukla, 1998).

History

The complex behavior of nonlinear oscillatory systems was observed long before dynamical chaos was understood. In fact, the possibility of complex behavior in dynamical systems was discovered by Henri Poincaré in the 1890s in his unsuccessful efforts to prove the regularity and stability of planetary orbits. Later on, experiments with an electrical circuit by van der Pol and van der Mark (1927) and the double-disk model experiments of the magnetic dynamo (Rikitake, 1958) also indicated the paradoxically complex behavior of a simple system. At that time, several mathematical tools were available to aid the description of the nontrivial behavior of dynamical systems in phase space, such as homoclinic Poincaré structures (homoclinic tangles). However, at the time, neither physicists nor mathematicians realized that deterministic systems may behave chaotically. It was only in the 1960s that the understanding of randomness was revolutionized as a result of discoveries in mathematics and in computer modeling (Lorenz, 1963) of real systems. An elementary model of chaotic dynamics was suggested by Boris Chirikov in 1959. During the last few decades, chaotic dynamics has moved from mystery to familiarity.

Standard Map and Homoclinic Tangle: The standard map (Chirikov, 1979) is an area-preserving map

$$\begin{aligned} I_{n+1} &= I_n + K \sin \Theta_n, \\ \Theta_{n+1} &= I_n + \Theta_n + K \sin \Theta_n, \end{aligned} \tag{12}$$

where Θ is an angle variable (computed modulo 2π) and k is a positive constant. This map was proposed as a model for the motion of a charged particle in a magnetic field. For K larger than K_{cr} , map

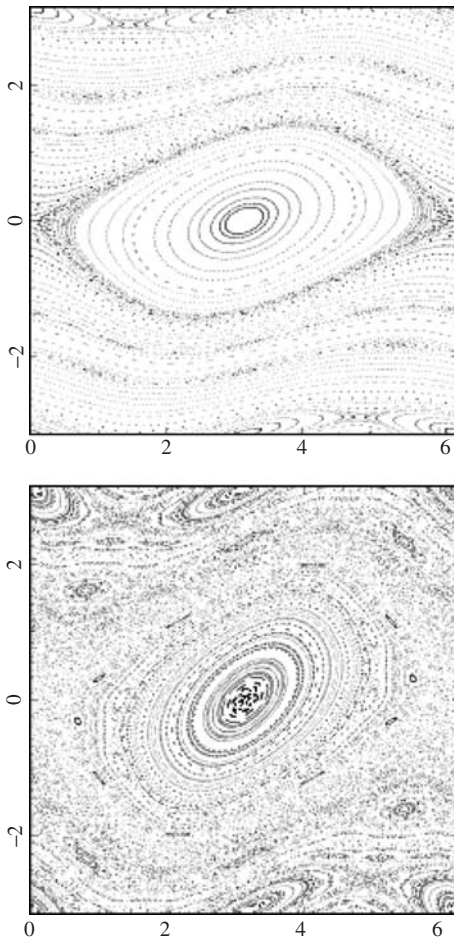


Figure 9. Examples of chaos in the standard map for two different values of K . The coexistence of the “chaotic sea” and “regular islands” that one can see in the panel on the right is typical for Hamiltonian systems with chaotic regimes (Lichtenberg & Lieberman, 1992).

(12) demonstrates an irregular (chaotic) motion; see Figure 9. The complexity of the phase portrait of this map is related to the existence of *homoclinic tangles* formed by stable and unstable manifolds of a saddle point or saddle periodic orbits when the manifolds intersect transversally. The complexity of the manifold’s geometry stems from the fact that, if stable and unstable manifolds intersect once, then they must intersect an infinite number of times. Such a complex structure results in the generation of a horseshoe mapping, which persistently stretches and then folds the area around the manifolds generating a chaotic motion. The layers of the chaotic motion are clearly seen in Figure 9.

Lorenz System: The first clear numerical manifestation of chaotic dynamics was obtained in the Lorenz model. This model is a three-dimensional dynamical system derived from a reasonable simplification of the fluid dynamics equations for thermal convection in a liquid layer heated from below. The differential equations $\dot{x} = \sigma(y - x)$, $\dot{y} = rx - y - xz$, $\dot{z} = -bz + xy$

are written for the amplitude of the first horizontal harmonic of the vertical velocity (x), the amplitude of the corresponding temperature fluctuation (y), and a uniform correction of the temperature field (z) (Lorenz, 1963). σ is the Prandtl number, r is the reduced Rayleigh number, and b is a geometric factor. The phase portrait of the Lorenz attractor, time series, and the return mapping generated on the Poincaré cross section computed for $r = 28$, $\sigma = 10$, and $b = \frac{8}{3}$ are presented in Figure 10. A simple mechanical model illustrating the dynamical origin of oscillations in the Lorenz system is shown in Figure 11 (See **Lorenz equations**).

Definition of Chaos

As was shown above, dynamical chaos is related to unpredictability. For quantitative measurement of the unpredictability, it is reasonable to use the familiar characteristics *dimension* and *entropy*. These characteristics are independent: it is possible to generate a time series that has a high dimension and at the same time entropy equal to zero. This is a quasi-periodic motion. It is also simple to imagine a low-dimensional dynamical system with high entropy (see, e.g., the map in Figure 3).

Various definitions of chaos exist, but the common feature of these definitions is the sensitive dependence on initial conditions that was formalized above as positive entropy. Thus, dynamical chaos is the behavior of a dynamical system that is characterized by finite positive entropy.

Chaotic Attractors and Strange Attractors

A region in the phase space of a dissipative system that attracts all neighboring trajectories is called an attractor. An attractor is the phase space image of the behavior established in the dissipative system, for example, a stable limit cycle is the image of periodic oscillations. Therefore, the image of chaotic oscillations is a chaotic attractor.

A *chaotic attractor* (CA) possesses the following two properties that define any attractor of the dynamical system:

- There exists a bounded open region U containing a chaotic attractor ($CA \in U$) in the phase space such that all points from this neighborhood converge to a chaotic attractor when time goes to infinity.
- A chaotic attractor is invariant under the evolution of the system,

In addition, the motion on a chaotic attractor has to be chaotic, for example:

- each trajectory of a chaotic attractor has at least one positive Lyapunov exponent.

Such types of attractors represent some regimes of chaotic oscillations generated by a Lorenz system and

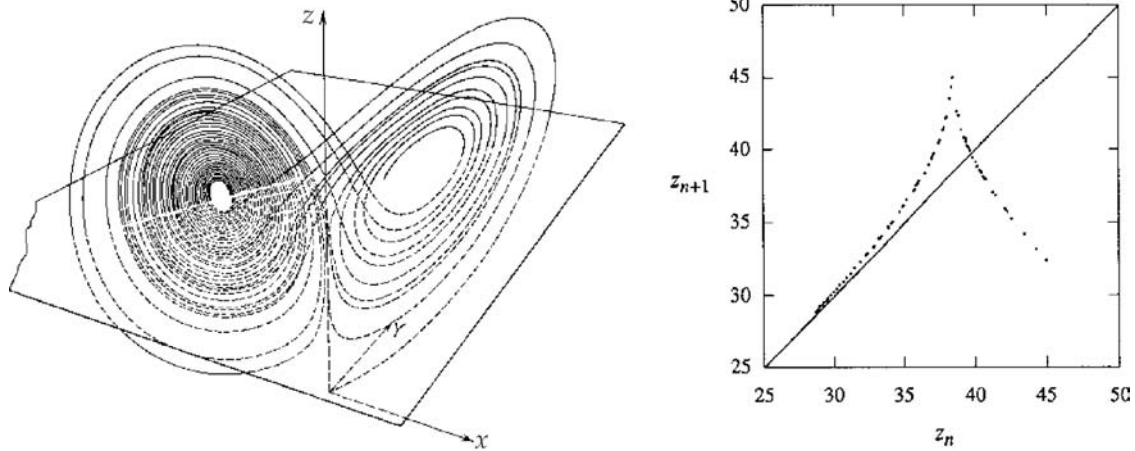


Figure 10. Lorenz attractor (left) and the return map $z_{n+1} = F(z_n)$ plotted for maximum values of variable z for the attractor trajectory (right).

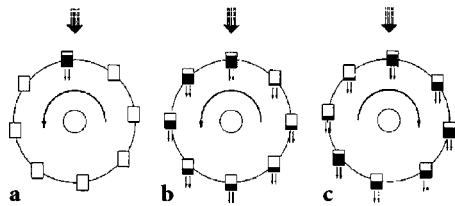


Figure 11. A toy model invented by Willem Malkus and Lou Howard illustrates dynamical mechanisms analogous to oscillations and chaos in the Lorenz system. Water steadily flowing into the top (leaky) bucket makes it heavy enough to start the wheel turning. When the flow is large enough, the wheel can start generating chaotic rotations characterized by unpredictable switching of the rotation direction; see Strogatz (1994, p. 302) for details.

the piece-wise linear maps. However, most of the chaotic oscillations observed in dynamical systems correspond to attractors that do not precisely satisfy the latter property. Although almost all trajectories in such attractors are unstable, some stable periodic orbits may exist within the complex structure of unstable trajectories. Chaos in such systems is persistent both in physical experiments and in numerical simulations because all of these stable orbits have extremely narrow basins of attraction. Due to natural small perturbations of the system, the trajectory of the system never settles down on one of the stable orbits and wanders within the complex set of unstable orbits.

The definition of a *strange attractor* is related to the complicated geometrical structure of an attractor. A strange attractor is defined as an attractor that cannot be presented by a union of the finite number of smooth manifolds. For example, an attractor whose topology can be locally represented by the direct product of a Cantor set to a manifold is a strange attractor. In many cases, the geometry of a chaotic attractor satisfies the definition of a strange attractor. At the same time, the definition of a strange attractor can be satisfied in the case of a nonchaotic strange attractor. This is an

attractor that has fractal structure, but does not have positive Lyapunov exponents.

The origin of chaotic dynamics in dissipative systems and Hamiltonian systems in many cases is the same and is related to coexistence in the phase space of infinitely many unstable periodic trajectories as a part of homoclinic or heteroclinic tangles.

The Lorenz attractor, as for many other attractors in systems with a small number of degrees of freedom, can appear through a finite number of easily observable bifurcations. The bifurcation of a sudden birth and death of a strange attractor is called a crisis. Usually, it is related to the collision of the attractor with an unstable periodic orbit or its stable manifold (Arnold et al., 1993; Ott, 1993).

Order in Chaos

How does the dynamical origin imprint in chaos? Or in other words, how can the rules or order of the dynamical system be found inside a chaotic behavior? Consider the images (portraits) of the dynamical chaos shown in Figures 7, 8, and 10. The elegance of these images reflects the existence of order in dynamical chaos.

The dynamical origin of such elegance is very similar: different trajectories with close initial conditions have to be close in time $t_l \approx 1/\lambda$, where λ is the maximally positive Lyapunov exponent. The domain occupied by the strange attractor in phase space is finite; thus, the divergence of the phase space flow changes to convergence, and as a result of sequential action of divergence and convergence of the phase flow in the finite domain, the mixing of trajectories occurs. Such mixing can be illustrated with the motions of liquids in the physical space experimentally observed by Ottino (1989; see Figure 1).

Another way to recognize the existence of order in chaos is to analyze its dependence on a control parameter. The macroscopic features of real stochastic



Figure 12. Appearance of spatiotemporal chaos in the extended Faraday experiment: chaotic patterns on the surface of the liquid layer in the oscillating gravitational field. The irregular chain of the localized structures—dark solitons—can be seen beneath a background of the square capillary lattice (Gaponov-Grekhov & Rabinovich, 1988).

processes, for example, Brownian motion or developed turbulence, depend on this parameter and change without any revolutionary events such as bifurcations. But for dynamical chaos, the picture is different. A continuous increase of control parameters of the logistic map does not necessarily gradually increase the degree of chaos: within chaos, there are windows—intervals of control parameter values in which the chaotic behavior of the system changes to stable periodic behavior, see Figure 4.

In a spatially extended system, for example, in convection or Faraday flow, order within chaos is related to the existence of coherent structures inside the chaotic sea (Rabinovich et al., 2001); see Figure 12.

Spatiotemporal Chaos

Similar to regular (e.g., periodic) motions, low-dimensional chaotic behavior is observed not only in simple (e.g., low-dimensional) systems but also in systems with many, and even with infinite number of degrees of freedom. The dynamical mechanisms behind the formation of low-dimensional chaotic spatiotemporal patterns in dissipative and nondissipative systems are different. In conservative systems, such patterns are related to the chaotic motion of particle-like localized structures. For example, a soliton that is described by a nonlinear Schrödinger equation with the harmonic potential

$$i \frac{\partial a}{\partial t} + \beta \frac{\partial^2 a}{\partial x^2} + (|a|^2 + \alpha \sin qx) a = 0 \quad (13)$$

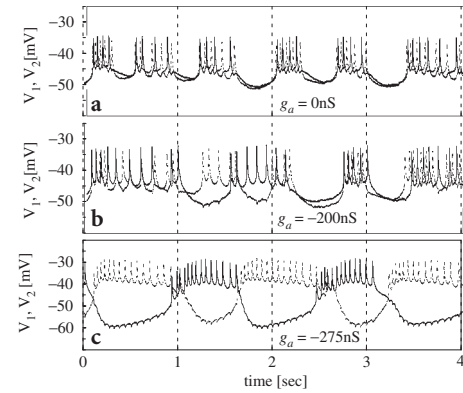


Figure 13. Dynamics of chaotic bursts of spikes generated by two living neurons coupled with an electrical synapse—a gap junction (Elson et al., 1998). Chaotic bursts in naturally coupled neurons synchronize (a). When natural coupling is compensated by additional artificial coupling g_a , the chaotic oscillations are independent oscillations (b). The neurons coupled with negative conductivity fire in the regimes of antiphase synchronization (c).

moves chaotically in physical space x and reminds us of the chaotic motion occurring in the phase space of a parametrically excited conservative oscillator (the equations of such an oscillator can be derived from (13) for slow variables characterizing the motion of the soliton center mass).

The interaction of the localized structures (particles) in a finite area, large in comparison with the size of the structure, can also lead to the appearance of spatiotemporal chaos. It was observed that collisions of solitons moving in two-dimensional space result in chaotic scattering similar to the chaotic motion observed in billiards (Gorshkov et al., 1992).

In dissipative nonlinear media and high-dimensional discrete systems, the role of coherent structures is also very important (such as defects in convection, clusters of excitations in neural networks, and vortices in the wake behind a cylinder; see Rabinovich et al., 2001). However, the origin of low-dimensional chaotic motions in such systems is determined by dissipation. There are two important mechanisms of finite dynamics (including chaos) that are due to dissipation: (1) the truncation of the number of excited modes (in hydrodynamic flows) due to high viscosity of the small-scale perturbations and (2) the synchronization of the modes or individual oscillators. Dissipation makes synchronization possible not only among periodic modes or oscillators but even in the case when the interacting subsystems are chaotic (Afraimovich et al., 1986). Figure 13 illustrates the synchronization of chaotic bursts of spikes observed experimentally in two coupled living neurons. In the case of a dissipative lattice of chaotic elements (e.g., neural lattices or models of an extended autocatalytic chemical reaction), complete synchronization leads to the onset

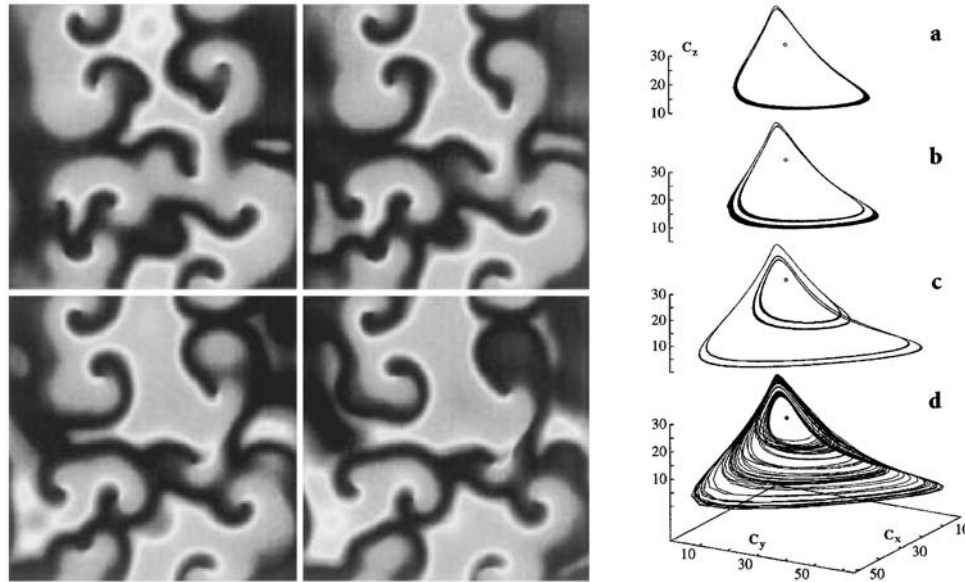


Figure 14. Coherent patterns generated in the chaotic medium with Rössler-type dynamics of medium elements. Left: an example of coherent patterns with defects. Right: evolution of the attractor with increasing distance r from a defect. The attractor changed from the limit cycle of period T at $r = r_1$ to the period $2T$ limit cycle at $r = r_2 > r_1$, then to the period $4T$ limit cycle at $r = r_3 > r_2$, and finally to the chaotic attractor for $r = r_4 > r_3$ (Goryachev & Kapral, 1996).

of a spatially homogeneous chaotic state. When this state becomes unstable against spatial perturbations, the system moves to the spatiotemporal chaotic state. A snapshot of such spatiotemporal chaos, which is observed in the model of chaotic media consisting of diffusively coupled Rössler-type chaotic oscillators, is presented in Figure 14. Figure 14 also illustrates the sequence of period-doubling bifurcations that are observed in the neighborhood of the defect in such a medium.

Edge of Chaos

In dynamical systems with many elements and interconnections (e.g., complex systems), the transition between ordered dynamics and chaos is similar to phase transitions between states of matter (crystal, liquid, gas, etc.). Based on this analogy, an attractive hypothesis named “edge of chaos”(EOC) appeared at the end of the 1980s. EOC suggests a fundamental equivalence between the dynamics of phase transitions and the dynamics of information processing (computation). One of the simplest frameworks in which to formulate relations between complex system dynamics and computation at the EOC is a cellular automaton. There is currently some controversy over the validity of this idea (Langton, 1990; Mitchel et al., 1993).

Chaos and Turbulence

The discovery of dynamical chaos has fundamentally changed the accepted concept of the origin of hydrodynamic turbulence. When dealing with turbulence at finite Reynolds number, the main point of interest is

the established irregular motion. The image of such irregularity in the phase space could be a chaotic attractor. Experiments in closed systems, for example, one in which fluid particles continuously recirculate through points previously visited, have shown the most common scenarios for the transition to chaos. These are (i) transition through the destruction of quasiperiodic motion that was observed in Taylor–Couette flow (Gollub & Swinney, 1975); (ii) period-doubling sequence observed in Rayleigh–Bénard convection (Libchaber & Maurer, 1980); and (iii) transition through intermittency (Gollub & Benson, 1980). Observation of these canonical scenarios for particular flows proved the validity of the concept of dynamical origin of the transition to turbulence in closed systems. It is possible to reconstruct a chaotic set in the phase space of the flow directly from observed data; see Brandstätter et al. (1982). At present it is difficult to say how dynamical chaos theory can be useful for the understanding and description of the developed turbulence.

The discovery and understanding of chaotic dynamics have important applications in all branches of science and engineering and, in general, to our evolving culture. An understanding of the origins of chaos in the last decades has produced many clear and useful models for the description of systems with complex behavior, such as the global economy (Barkly Russel, 2000), the human immune system (Gupta et al., 1998), animal behavior (Varona et al., 2002), and more. Thus, chaos theory provides a new tool for the unification of the sciences.

M.I. RABINOVICH AND N.F. RULKOV

See also **Attractors; Billiards; Butterfly effect; Chaos vs. turbulence; Controlling chaos; Dripping faucet; Duffing equation; Entropy; Fractals; Hénon map; Horseshoes and hyperbolicity in dynamical systems; Intermittency; Kicked rotor; Lorenz equations; Lyapunov exponents; Maps; Maps in the complex plane; Markov partitions; Multifractal analysis; One-dimensional maps; Order from chaos; Period doubling; Phase space; Quasiperiodicity; Rössler systems; Routes to chaos; Sinai–Ruelle–Bowen measures; Spatiotemporal chaos; Synchronization; Time series analysis**

Further Reading

- Abarbanel, H.D.I. 1996. *Analysis of Chaotic Time Series*, New York: Springer
- Afraimovich, V.S., Verichev, N.N. & Rabinovich, M.I. 1986. Stochastic synchronization of oscillations in dissipative systems. *Izvestiya Vysshikh Vchebnykh Zavedenii Radiofizika. RPOAEC*, 29: 795–803
- Arnold**, V.I., Afraimovich, V.S., Ilyashenko, Yu.S. & Shilnikov, L.P. 1993. Bifurcation theory and catastrophe theory. In *Dynamical Systems*, vol. 5, Berlin and New York: Springer
- Barkly Russel, J., Jr. 2000. *From Catastrophe to Chaos: A General Theory of Economic Discontinuities*, 2nd edition, Boston: Kluwer
- Brandstätter, A., Swift, J., Swinney, H.L., Wolf, A., Doyne Farmer, J., Jen, E. & Crutchfield, P.J. 1982. Low-dimensional chaos in a hydrodynamic system. *Physical Review Letters*, 51: 1442–1445
- Chirikov, V.A. 1979. A universal instability of many-dimensional oscillator systems. *Physics Reports*, 52: 264–379
- Deco, G. & Schürmann, B. 2000. *Information Dynamics: Foundations and Applications*, Berlin and New York: Springer
- Elson, R.C., Selverston, A.I., Huerta, R., Rulkov, N.F., Rabinovich, M.I. & Abarbanel H.D.I. 1998. Synchronous behavior of two coupled biological neurons. *Physical Review Letters*, 81: 5692–5695
- Gaponov-Grekhov, A.V. & Rabinovich, M.I. 1988. *Nonlinearity in Action: Oscillations, Chaos, Order, Fractals*, Berlin and New York: Springer
- Gollub, J.P. & Benson, S.V. 1980. Many routes to turbulent convection. *Journal of Fluid Mechanics*, 100: 449–470
- Gollub, J.P. & Swinney, H.L. 1975. Onset of turbulence in rotating fluid. *Physical Review Letters*, 35: 927–930
- Gorshkov, K.A., Lomov, A.S. & Rabinovich, M.I. 1992. Chaotic scattering of two-dimensional solitons. *Nonlinearity*, 5: 1343–1353
- Goryachev, A. & Kapral, R. 1996. Spiral waves in chaotic systems. *Physical Review Letters*, 76: 1619–1622
- Gupta, S., Ferguson, N. & Anderson, R. 1998. Chaos, persistence, and evolution of strain structure in antigenically diverse infectious agent. *Science*, 280: 912–915
- Langton, C.C. 1990. Computation at the edge of chaos—phase transitions and emergent computation. *Physica D*, 42: 12–37
- Libchaber, A. & Maurer, J. 1980. Une expérience de Rayleigh-Bénard en géométrie réduite; multiplication, accrochage et démultiplication de fréquences. *Journal de Physique Colloques*, 41: 51–56
- Lichtenberg, A.J. & Leiberman, M.A. 1992. *Regular and Chaotic Dynamics*, Berlin and New York: Springer
- Lorenz, E.N. 1963. Deterministic nonperiodic flow. *Journal of Atmospheric Science*, 20: 130–136
- Mitchel, M., Hraber, P. & Crutchfield, J. 1993. Revisiting the edge of chaos: evolving cellular automata to perform computations. *Complex Systems*, 7: 89–130
- Murray, N. & Holman, M. 1999. The origin of chaos in the outer solar system. *Science*, 283: 1877–1881
- Ott, E. 1993. *Chaos in Dynamical Systems*, Cambridge and New York: Cambridge University Press
- Ottino, J.M. 1989. *The Kinetics of Mixing: Stretching, Chaos, and Transport*, Cambridge and New York: Cambridge University Press
- Pikovsky, A.S. & Rabinovich, M.I. 1978. A simple generator with chaotic behavior. *Soviet Physics Doklady*, 23: 183–185 (see also Rabinovich, M.I. 1978. Stochastic self-oscillations and turbulence. *Soviet Physics Uspekhi*, 21: 443–469)
- Rabinovich, M.I., Ezersky, A.B. & Weidman, P.D. 2001. *The Dynamics of Patterns*, Singapore: World Scientific
- Rikitake, T. 1958. Oscillations of a system of disk dynamos. *Proceedings of the Cambridge Philosophical Society*, 54: 89–105
- Roux, J.C., Simoyi, R.H. & Swinney, H.L. 1983. Observation of a strange attractor. *Physica D*, 8: 257–266
- Shukla, J. 1998. Predictability in the midst of chaos: a scientific basis for climate forecasting. *Science*, 282: 728–731
- Sinai, Ya.G. 2000. *Dynamical Systems, Ergodic Theory and Applications*, Berlin and New York: Springer
- Strogatz, S.H. 1994. *Nonlinear Dynamics and Chaos: With Applications to Physics, Biology, Chemistry, and Engineering* Reading, MA: Addison-Wesley
- Takens, F. 1991. Chaos, In *Structures in Dynamics: Finite Dimensional Deterministic Studies*, edited by H.W. Broer, F. Dumortier, S.J. van Strien & F. Takens, Amsterdam: North-Holland Elsevier Science
- Ueda, Y. 1992. *The Road to Chaos*, Santa Cruz, CA: Aeirial Press
- van der Pol, B. & van der Mark, B. 1927. Frequency demultiplication. *Nature*, 120: 363–364
- Varona, P., Rabinovich, M.I., Selverston, A.I. & Arshavsky, Yu.I. 2002. Winnerless competition between sensory neurons generates chaos: A possible mechanism for molluscan hunting behavior. *CHAOS* 12: 672–677
- Young, L.S. 1998. Developments in chaotic dynamics. *Notices of the AMS*, 17: 483–504

CHARACTERISTICS

The Method of Characteristics

Systems of first-order partial differential equations describe many different physical phenomena from the behavior of fluids, gases, and plasmas. To introduce the Method of Characteristics, consider the simple scalar conservation law of the form

$$\frac{\partial U}{\partial t} + A(U) \frac{\partial U}{\partial x} = 0. \quad (1)$$

Here, $U = U(x, t)$, where x is a spatial coordinate and t is the time coordinate. The function $A(U)$ defines the speed of propagation of a disturbance and either may be independent of U , in which case equation (1) is a linear partial differential equation, or it may depend explicitly on the dependent variable U , in which case the equation is a nonlinear partial differential equation.